Communications on Applied Nonlinear Analysis
ISSN: 1074-133X
Vol 32 No. 2s (2025)

# Single-Phase Multilevel Inverter Design with Low Voltage Stress and Optimized Control Model

**Dr. Vijayalaxmi Biradar[1], Ikhar Avinash Khemraj[2]**

[1,2]Department Of Electrical And Electronics Engineering, Kalinga University, Raipur, India

***Article History:***

***Received:*** *30-08-2024*

***Revised:*** *11-10-2024*

***Accepted:*** *28-10-2024*

**Abstract:**

The research explicitly examines the power control of a single-phase renewable energy sources battery energy storage system (RES-BESS)mixed-distributing network designed for domestic usage. The system utilizes a cascaded H-bridge (CHB) conversion architecture as its grid connection. The CHB uses a hierarchical power management design consisting of a single centralized regulator for the top layer and several dispersed regulators for the bottom layer. The higher stratum produces the reference signals that need to be monitored. Under optimal circumstances, the CHB should operate efficiently with all solar panels at their Maximum Power Point (MPP) and with an electrical factor of 1. However, several functional limitations prevent this from always being feasible, such as limits related to voltage and current, biased shadowing, and State of Charge (SOC) incompatibilities. Hence, a novel optimization technique is introduced to take into account these impacts directly and calculate a collection of reference parameters to be monitored. This approach aims to maximize the long-term viability of the structure while ensuring compliance with the given limitations. The optimization method in this structure incorporates many functional needs, prioritizing them based on the specific operating circumstances. The decentralized management layer utilizes traditional feedback-controlling methods to monitor the best referencing. Experimental findings are conducted to verify the best method under normal conditions for operation and evaluate the efficacy of the suggested CHB arrangement with the complete control technique.

**Keywords:** Multilevel Inverter, Cascaded H-Bridge, Optimisation, Low Voltage Stress.

## 1. Need for Renewable Energy Sourcesand multilevel inverters

They are integrating Renewable Energy Sources (RES) into the conventional electricity grids [1]. The significant integration of RES, which is highly unpredictable, has fundamentally altered the grid framework and presented novel obstacles for the power electronic conversions linked to the grid. The flexibility of RES has given rise to the notion of Distributing Electricity Resources (DER): decentralized electricity generation facilities and energy storing facilities dispersed among the electrical grids and situated near end-users [2]. Solar photovoltaic plants have seen significant expansion in the last ten years, mainly owing to incentives implemented by local authorities and the substantial cost reduction from technological advancements [3].

A vital obstacle created by the widespread integration of dispersed PV electricity supplies into the conventional electrical network is the sporadic characteristic and substantial shadowing occurrences of the provided electricity. Combining Energy Storing Systems (ESS) with RES is considered the most recognized option to address and surmount the issues above [4].Severe network intrusions may result from anomalies in firewall rules, including the unauthorized passage of malicious user into a

subnetwork or the omission of legitimate traffic, both of which may impede the proper operation of users[5].

Batteries have become more popular and widely used in various ESS. This is primarily due to their capacity to provide scalable power ratings, affordability, lack of pollution, and higher dependability levels. A Battery ESS (BESS) is a power reservoir in PV production and provides more benefits [22]. Initially, it improves the use of energy generated by residential photovoltaic (PV) systems by keeping excess power during shortages and delivering it when needed [6]. It offers multiple features to the electric grids, such as voltage and frequency management and demand shifting.

Incorporating a dispersed energy storage system enables the equalization of the power output from each sub-module and the mitigation of the fluctuations in the power supplied to the grid. These mixed RES-BESS systems enable more efficient use of DER, optimize the allocation of PV resources, boost the overall system's effectiveness and safety, and offer a flexible and uninterrupted power supply in the event of a breakdown.The paper [7] shows that the problem considered is related to one of the forms of Boolean Matrix Factorization.

Multi-Level Inverters (MLIs)are extensively used in different areas, such as renewable energy converting structures, motor drive uses, Uninterruptible Power Supply (UPS) structures, induction heating structures, dispersed generations, and high-voltage DC structures. This is primarily due to their appealing attributes, including enhanced reliability of power, electromagnetic features, and decreased energy loss. Switched-capacitor MLIs (SCMLIs) are prevalent MLIs in cascaded H-bridge [8,25]. Using the specified input supply might decrease the conversion's size and expense. Extra circuits are required for voltage equalization of the capacitance. It is essential to have a converter with minimal electrical power sources and self-balanced capacitance to get elevated voltage increments while using a smaller quantity of gadgets.For data clustering, four discrete various pre-trained models are utilized. In addition, a novel model was suggested, which had been trained using the provided datasets [9]. Through an evaluation of a combined technology and an expansion of the existing C-ITS standards, this article offers a comprehensive overview of how the concept of IoT might converge with the C-ITS domain, based on interim results published by the authors [10].

The following sections are arranged in the specified manner: Section 2 pertains to the background information and relevant research. Section 3 proposes the design of a single-phase multilevel inverter that minimizes voltage stress. Section 4 examines the outcomes of experimental discoveries. Section 5 closes by presenting the discussion and results of the research.

## 2. Related works

In the CHB conversion combined with BESS, the energy-storing instrument is often positioned in parallel with the PV system for every sub-module. This arrangement allows for the controlled injection of actual and reactive energy into the electrical grid—further converters are required to facilitate energy storage in the units. The low cost of equipment is appealing. Nevertheless, several studies have concentrated on CHB-based BESS throughout the last few decades because the packs of batteries also function as low-voltage direct current (DC) suppliers [21]. A significant number of them have suggested the use of distributed electricity control. The authors proposed a hierarchical dispersed control construction comprising central control for power supply monitoring, additional

control utilizing a consensus method to govern power distribution among components, and energy state of charge (SOC) managing to enhance the effectiveness of BESS [23]. A carrier phase shifting method was developed to accomplish multilayer voltage and harmonic decrease.

Nevertheless, the suggested arrangement should have included the control of PV sources [11]. The researchers suggested a complete hardware design for a PV-CHB Converter with a BESS. Every component comprises a dual-stagephotovoltaic and BESS using power conversions for every step [12]. This enabled the surpassing of the operational constraints of PV-CHB systems. The authors suggested integrating photovoltaic components and BESS into the DC connection of everyCHB conversion [13].

The authors provide a method for managing power specifically for a concentrated form of BESS consisting of an n-PV module and one BESS unit [14]. A revised power control technique was devised to dynamically adjust PV panels' present electrical power levels, shifting them away from their optimum. This was done to address the issue of excessive modulation resulting from repeated battery charging and discharge.

SCMLIs can achieve voltage gain more significantly than one via their modular construction [15]. A transmitted Multilevel Inverter (MLI) is constructed using single-stage switched-capacitor components [16]. The topology obviates the need for the CHB and maintains a reduced blocking supply, in contrast to several comparable endeavors. The design requires substantial power toggles, capacitors, and input energy sourcesto provide a high step voltage at the output. A novel high-gain configuration, including self-voltage managing, is introduced [17]. Condensers are charged during the first two phases and released during the subsequent phasesto produce the MLI power. A series link of fundamental components is also implemented to enhance the number of phases.

MLI's proposed step-up voltages have fewer switches and can self-balance [18]. It comprises a single capacitor, semiconductor diode, and power controls. The electrical components are charged and released during each cycle via a series or parallel link. A novel step-up configuration using a solitary direct energy source has been implemented [19]. SDS has gained increasing popularity in recent years, prompting numerous companies to introduce their own products. However, a universally applicable standard has yet to materialize; the majority of products are only compatible with their respective devices, and SDS can only incorporate a limited number of storages [26].To get a 13-level output voltage, it is necessary to use a trio of capacitors along with 13 electrical switches and a pair of diodes. The circuit configuration necessitates using nine electrical switches, one direct current source, two capacitors, and two diodes to achieve a nine-level output in the converters [20]. To provide a more excellent range of voltage options, the MLI capacitors can be charged using a non-symmetrical way that relies on an enhanced series/parallel approach.

## 3. Proposed single-phase multilevel inverter design with low voltage stress

The configuration of the RES-BESS employing the CHB conversion can be seen in Fig. 1. The photovoltaic and battery packs are linked to the complete H-bridge energy sub-modules Low Voltage (LV) DC bus in this setup. The voltage and power of PV panels fluctuate in response to solar radiation to optimize the power output. The variation results from changes in the SOC and the flow of electricity through the resistance inside the modules. The energy sub-module, equipped with a

battery, functions as a storage device to offset the disparity between the electricity generated by the photovoltaics and the electricity that has to be sent to the system. A two-layer controlling design is suggested to regulate the electrical flow at the converting link and the energy in every sub-component.

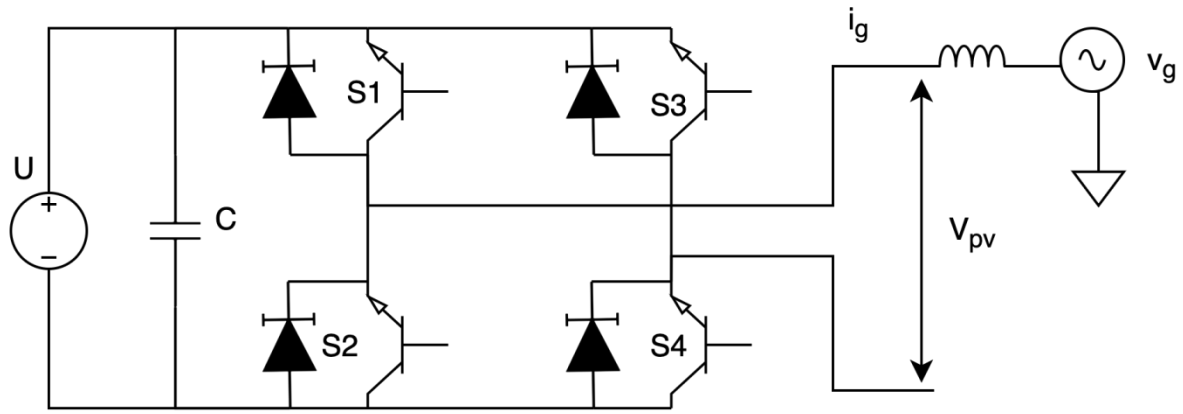


Fig. 1. CHB inverter design

- Upper layer

The system comprises a central controller responsible for calculating the standard electricity on the AC component of the CHB converter. It ensures that the various sub-components battery charging status and the most significant energy and electricity are within the specified limits. At this stage, the primary electrical measurements of each sub-module (such as SOC, voltage, and PV power data) are gathered via a Fieldbus system. A linear loop and forwarding controller are then used to regulate the AC grid electricity.

- Lower layer

The system comprises local controllers installed in each sub-module, which are responsible for executing the Maximum Power Point Tracking (MPPT) for photovoltaic components and managing the charging/discharging regulation of the battery. The standard electricity for every sub-component is determined based on the collective AC voltage standard computed by the central controller and the stockAC voltages derived by the linear loop and feed-forward regulators of PV energies for every sub-module. Pulse Width Modulation (PWM) controls the total bridge conversions to achieve a specific AC output.

The PWM was achieved using a standard reference analysis. Yet, this assessment is performed independently for the PV-fed and battery-fed stacking—various modulation strategies used for multi-level conversion. TheLS and Phase Shifting (PS) methods contrast Yeg and Yoea's standard variables with many carriers and create the appropriate outputs to control the components.

The modulation is readily adjusted to account for power flow control between various components explicitly. The PV-fed stack uses this feature to offset the uneven distribution of radiation across various PV-fed components. Panels with greater radiation levels are usually required to generate more electricity, resulting in a larger power output from these screens.

Similarly, the electricity regulation of the BESS-fed stackingis efficiently utilized to balance the SOC of multiple Multi-Module Converter (MMC) modules.Energy optimization in various MMC components is achieved using algorithmic sorting for LS-based modulating methods and additional divergent mode power injectors for PS-based modulating methods.

### 3.1 Inverter topology

The suggested 33-level MLI designs are carried out as the basic unit and the broader expanded architecture. The design formulas, switching indicates, loading current routes, Maximal Blocked Voltages (MBV), and Total Standing Voltages(TSV) computations are used to determine various aspects of the MLI, such as the standard output voltage waveforms. Different MLI variables are computed to gauge the efficacy of MLI.

The system consists of eight unidirectional and four reversible semiconductor shifts, each connected to four input DC voltage generators. The fundamental component of the suggested design can produce thirty-three distinct voltages at its final state. The input DC power supplies P1, P2, P3, and P4 have magnitudes chosen in a proportion of 1:2:4:9, with a $V_{DC}$ value of 25V.

The converter is well-suited for usage in renewable energy-producing systems that contain a diverse range of DC sources, thanks to its ability to handle various inputs from different sources. In real-world situations, such as solar-generating systems, DC-to-DC conversions are used to integrate PV cells to maximize the shape of the waveform of the outgoing voltage.

The number of needed DC supplies ($N_{dc}$) is theoretically determined by the equation relating to the number of levels ($N_L$) employed and expressed in Eqn. (1).

$$N_{dc} = \frac{N_L - 7}{5} \quad (1)$$

The needed number of controls, $N_{SW}$, is statistically correlated to the number of stages, $N_L$, via Eqn. (2).

$$N_s = \frac{N_L - 7}{2} \quad (2)$$

The gate driving circuitry $N_{gd}$ that are necessary are provided by Eqn. (3).

$$N_{gd} = \frac{N_L + 4}{3} \quad (3)$$

The maximum voltage results, denoted as $V_{0,max}$, is determined by Eqn. (4).

$$V_{0,max} = \frac{N_L - 1}{2} \quad (4)$$

Two switching modes result in an output voltage of zero. The fifth stage is employed during the initial portion of the modified sine wave, and the sixth stage is utilized during the latter portion. Switching S1 and S2, as well as S3 and S4, are mutually complimentary. A pause is included between these switches' changes to prevent an electrical short's occurrence.

(1) State-1

The stream of electric current originates from the positive end of the DC supply and passes through switching 1. It then travels via the loading and completes the circuit by connecting to the opposing end of the DC supply via S4. A direct current voltage is present at the load station.

(2) State-2

Electric current originates from the positive end of the DC supply and moves towards S1. It then travels across the demand and connects the circuit at the neutral position, connecting both DC link capacitances via S3. In its current condition, the diode of S2 exhibits behavior similar to that of an upward-biased diode, allowing the flow of electricity. The loading terminal exhibits a DC voltage of $V_{DC}$/2 in this condition.

(3) State-3

The pace of electric current originates from the positive end of the DC origin, passes through S3, and then proceeds via the adverse potentialof the demand that is being powered. The circuit is completed by returning to the opposing end of the DC source via S 2. The final result exhibits a negative polarity (-$V_{DC}$) voltage.

(4) State-4

The load's positive connection is linked to the neutral position across the DC link capacitor via S1 and S3's diode. In contrast, the load's negative terminals are connected to the source's negative endpoint inputs via S2. In this position, the diode of S2 will exhibit a forward bias. A voltage of -$V_{DC}$/2 is generated across the loading connections.

(5) State-5

S1 and S3 must be turned on concurrently to achieve zero voltage at the load connections. As a result, the load connections will be connected directly, causing the possible variance across them to become zero. In future generations, the converter will utilize the zero regions in a mode known as "inconsistent convection," allowing it to minimize the dimensions of the resultant passive filter.

(6) State-6

Itprovides zero voltage by activating S2 and S4. Additionally, it will cause the voltage variation in the result to become zero. The suggested topology efficiently utilizes both states 5 and 6. This is used during the positive phase of the modified sine wave, whereas state 6 is activated by the inverter during the reverse phase of the modulating sine wave, as required. Switching between stages 5 and 6 within a single cycle of a modified sine wave decreases the strains on the voltage change rate (dv/dt) during the switching process.

3.2 Controller Design for MLI

The multilevel inverting controllers are designed using a modulating waveform. It demonstrates the stacking of four triangle carrier messages with the harmonic modulating message of the required output frequencies to control the PWM message's outcome. Figure 2 depicts the segmentation of the modified sine wave into four distinct regions.

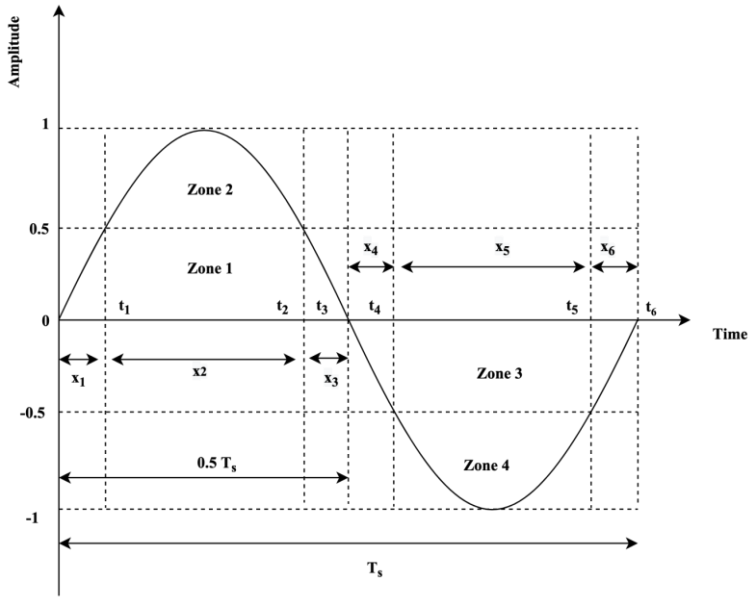


Fig. 2. Modulation signal of the control output

- The switched signal alternates among stages 2 and 6 inside the first section of the modulating wave.
- States 1 and 2 are employed in the second portion of the modulating wave to create the changing signal.
- The switched signal generated in the third portion alternates between stages 4 and 5.
- During the concluding phase of the modulating wave, inputs will alternate among states 3 and 4 to produce gate impulses.

Using two different zero-voltage phases throughout the positive and negative phases of the modulating signal minimizes switched stresses and preserves the voltage equilibrium around the DC-link capacitance.

## 4. Experimental Outcomes

The effectiveness of the suggested technique has been confirmed by rigorous computations in the MATLAB surroundings, specifically for a real-time scenario. The high-frequency control activities, such as the Phase-Locked Loop (PLL), feedback current control, PWM, and DC estimate, were performed at 10 kHz. The optimization process was conducted at 25 Hz. The low-frequency activities, such as the MPPT of the photovoltaic-fed components and the state of charge estimate of the BESS-fed components, are performed at a frequency of 0.6 Hz. The evaluation conditionis selected to emphasize the nature of the method. The method begins from a state of equilibrium. The screens operate at their maximum peak power but receive different irradiation levels. The power output at their MPP is 1.4 kW for one panel and 1.6 kW for the other panel.

Three distinct tests were conducted to evaluate the implementation of grid electricity control. These tests include Balancing dispersion (Test I), Imbalancedispersion divided between electricity given by photovoltaic and battery energy (Test II), and extra Electricity kept in battery energy (Test III). The implementation of MPPT management for photovoltaic sources has yet to be carried out since the

primary objective is to evaluate the performance of photovoltaic supplies and battery energy under various dispersion conditions.

Table 1. Test I results

| Module | Voltage (V) | Current (A) | Power (W) | Power Quality (%) | Efficiency (%) |
|---|---|---|---|---|---|
| PV-1 | 34.4 | 1.32 | 41.5 | 14.2 | 94.1 |
| PV-2 | 34.7 | 1.53 | 52.6 | 21.4 | 73.4 |
| BESS-3 | 35.1 | 1.37 | 47.3 | 18.5 | 83.2 |
| BESS-4 | 35.6 | 1.53 | 51.4 | 21.3 | 74.6 |
| Grid | 47.5 | 3.54 | 162.4 | 61.3 | 81.5 |

The first test was conducted with a focus on achieving equitable operations among the cells. Table 1 presents the powers, current, electricity, power quality, and effectiveness of the various H-bridge components. All sources provide about equal amounts of electricity, but with varying levels of effectiveness. The grid receives a total power of 162.4 watts, with a total effectiveness of 81.5. The conversion voltage is derived from the DC supply observations and the switch signals to capture the modulation waveform with a broad bandwidth. Additionally, the voltage loss of gadgets (VCE= 1.53V) was considered.

Table 2. Test II results

| Module | Voltage (V) | Current (A) | Power (W) | Power Quality (%) | Efficiency (%) |
|---|---|---|---|---|---|
| PV-1 | 36.2 | 1.43 | 52.4 | 10.4 | 90.3 |
| PV-2 | 35.2 | 1.78 | 62.1 | 13.2 | 75.2 |
| BESS-3 | 37.6 | 1.21 | 38.5 | 8.4 | 81.4 |
| BESS-4 | 37.8 | 1.18 | 38.4 | 8.1 | 80.4 |
| Grid | 48.3 | 3.36 | 153.6 | 31.5 | 83.6 |

The second experiment was conducted with an uneven distribution of both PV and BESS modules while maintaining equal conditions within each module type. Table 2 displays power, electricity, voltages, power quality, and effectivenessacross the various H-bridge components. Each source yields varying amounts of energy with differing efficiency levels, havingits distributing gains. The AC cell values of the photovoltaic resources acquired using a modulating index of 0.52, while the BESS cells used a modulating value of 0.32. The power ratio of the output supply converter was 0.92. The grid receives a total power of 154 watts, with a total effectiveness of 83.6. The conversion energy is derived from the DC supply readings and the switched messages, as a capacity is required to capture the modulating waveforms accurately. The decrease in the voltage of gadgets was taken into account.

Table 3. Test III result analysis

| Module | Voltage (V) | Current (A) | Power (W) | Power Quality (%) | Efficiency (%) |
|---|---|---|---|---|---|
| PV-1 | 35.2 | 2.1 | 72.3 | 18.3 | 97.2 |
| PV-2 | 35.8 | 2.43 | 79.6 | 19.6 | 88.4 |

| | | | | | |
|---|---|---|---|---|---|
| BESS-3 | 36.9 | 2.63 | 105.2 | 26.4 | 68.5 |
| BESS-4 | 38.3 | -0.85 | -36.2 | -9.3 | 62.5 |
| Grid | 47.2 | 3.52 | 156.2 | 38.5 | 71.5 |

The third test was conducted to evaluate the battery charging state. The BESS-4is recharged when the batteries are exhausted and discharges when the batteries are recharged. The results are depicted in Table 3. The modulating signals are in stage, so charging two battery energysources could lead the photovoltaic-fed components to operate in over-modulating condition. Each cell generates varying amounts of power with variable levels of efficiency, taking into account their distributing gains and direct supply. The AC supplyof the solar power were measured using modulation indices of 0.82 and 0.84. The initial battery energy storagehad a modulating index of 0.84. However, the final cell of the BESS had a variation value of 0.57 since it was being recharged. The energy factor of the resultant supply converter is 0.82. The grid receives a total electrical supply of 154 watts with an overall effectiveness of 71.5. The total efficacy in this working state was lower than the others, as the BESS cells had values of 0.57 and 0.63 correspondingly. Therefore, the third cell, BESS-3, simultaneously provides power to the grid and the battery.

The present Total Harmonic Distortion value is around 13%. The modulating waveform in the above experiment does not exhibit the distinctive staircase shape often associated with multilevel inverters. The lack of apparent distinction between certain levels is attributed to a single output voltage in phase conflict with all of them. The DC voltages associated with the solar power plants exhibit significant instability compared to earlier scenarios, characterized by a distinct oscillation at 100 Hz. This is because the two cells are experiencing a higher level of demand but have yet to reach their MPP. As a result, the system is operating on the steepest part of the voltage-current typical curve.

## 5. Conclusion and findings

This article examines the electricity management approach of RES-BESS for residential applications, explicitly employing a single CHB inverter architecture. Under optimal circumstances, the methodmust operate using its maximum power with the CHB and all photovoltaic cells. Nevertheless, the system has limitations due to functional restrictions, making it impractical to always achieve the desired outcome. Hence, the energy administration approach addresses an optimum issue by minimizing the grid's reactive electricity, solar panels, and storage components while maximizing photovoltaic energy output. Incorporating the battery mitigates power fluctuations caused by the unpredictable nature of PV generation. The latter aims to mitigate short-term PV fluctuations by offering a dynamic ESS and synchronizing power generation and consumption. The suggested solution utilizes a control system design combining centralized and distributed components. This architecture has several priority tiers, including upper and lower levels. The steady-state voltages and standard supplyare determined by resolving a multi-objective optimizing issue. This issue has been formulated, considering the system's technical limitations and various functional demands. The priority stages of these needs vary depending on the translator's operation circumstances. The control solution utilized a technique that involves modeling the circuit using an alternative circuit. An experiment was carried out to demonstrate the operational boundaries of the

PV-BESS CHB design by varying the weights. The purpose was to illustrate how these limitations were surpassed. The robust system result shows the efficacy of the suggested design and management strategy. Asimulation prototype was used to demonstrate the practicality of the proposed CHB design and evaluate its overall effectiveness, considering the power supply limitations of the cells.

## References

[1] Dalala, Z., Al-Omari, M., Al-Addous, M., Bdour, M., Al-Khasawneh, Y., & Alkasrawi, M. (2022). Increased renewable energy penetration in national electrical grid constraints and solutions. Energy, 246, 123361.

[2] Caballero-Peña, J., Cadena-Zarate, C., Parrado-Duque, A., & Osma-Pinto, G. (2022). Distributed energy resources on distribution networks: A systematic review of modeling, simulation, metrics, and impacts. International Journal of Electrical Power & Energy Systems, 138, 107900.

[3] Narasimman, K., Gopalan, V., Bakthavatsalam, A. K., Elumalai, P. V., Shajahan, M. I., & Michael, J. J. (2023). Modeling and real-time performance evaluation of a 5 MW grid-connected solar photovoltaic plant using different artificial neural networks. Energy Conversion and Management, 279, 116767.

[4] Rana, M. M., Uddin, M., Sarkar, M. R., Meraj, S. T., Shafiullah, G. M., Muyeen, S. M., ... & Jamal, T. (2023). Applications of energy storage systems in power grids with and without renewable energy integration—A comprehensive review. Journal of Energy Storage, 68, 107811.

[5] Valenza, F., & Cheminod, M. (2020). An Optimized Firewall Anomaly Resolution. J. Internet Serv. Inf. Secur., 10(1), 22-37.

[6] Khezri, R., Mahmoudi, A., & Aki, H. (2022). Optimal planning of solar photovoltaic and battery storage systems for grid-connected residential sector: Review, challenges and new perspectives. Renewable and Sustainable Energy Reviews, 153, 111763.

[7] Saenko, I., & Kotenko, I.V. (2014). Design of Virtual Local Area Network Scheme Based on Genetic Optimization and Visual Analysis. Journal of Wireless Mobile Networks, Ubiquitous Computing, and Dependable Applications (JoWUA), 5(4), 86-102.

[8] Ullah, Atta, Kamal Shah, and Rahmat Ali Khan. "Series form solution to two dimensional heat equation of fractional order." Results in Nonlinear Analysis 2.4 (2020): 193-199.

[9] Lei, M., & Wang, Y. (2022). A Transformerless Railway Power Quality Compensator Based on a Cascaded H-Bridge Featuring Reduced Branch Capacity Requirement. IEEE Transactions on Power Delivery, 37(6), 5443-5453.

[10] Camgözlü, Y., & Kutlu, Y. (2023). Leaf Image Classification Based on Pre-trained Convolutional Neural Network Models. Natural and Engineering Sciences, 8(3), 214-232.

[11] Virág, L., Kovács, J., & Edelmayer, A. (2013). Interacting advanced ITS communications with low-power sensor networks. Journal of Wireless Mobile Networks, Ubiquitous Computing, and Dependable Applications (JoWUA), 4(3), 79-96.

[12] Weng, Shengquan. "Convergence theorems of modified Ishikawa iterations in Banach spaces." Results in Nonlinear Analysis 2.3 (2019): 125-135.

[13] Cai, Y., & Qi, D. (2022). A distributed VSG control method for a battery energy storage system with a cascaded H-bridge in a grid-connected mode. Global Energy Interconnection, 5(4), 343-352.

[14] Nguyen, T. T., Nguyen, T. T., & Le, B. (2022). Artificial ecosystem optimization optimizes battery energy storage systems' position and operational power on the distribution network considering distributed generations. Expert Systems with Applications, 208, 118127.

[15] Wang, Y., Ye, J., Ku, R., Shen, Y., Li, G., & Liang, J. (2023). A modular switched-capacitor multilevel inverter featuring voltage gain ability. Journal of Power Electronics, 23(1), 11-22.

[16] Jena, K., Kumar, D., Janardhan, K., Kumar, B. H., Singh, A. R., Nikolovski, S., & Bajaj, M. (2023). A Novel Three-Phase Switched-Capacitor Five-Level Multilevel Inverter with Reduced Components and Self-Balancing Ability. Applied Sciences, 13(3), 1713.

[17] Kumari, P., Singh, A. K., Kumar, N., & Mandal, R. K. (2023). Self-balanced high gain switched-capacitor boosting inverter with a lower cost function. International Journal of Electronics, 1-18.

[18] Islam, S., Siddique, M. D., Iqbal, A., & Mekhilef, S. (2022). A 9-and 13-level switched-capacitor-based multilevel inverter with enhanced self-balanced capacitor voltage capability. IEEE Journal of Emerging and Selected Topics in Power Electronics, 10(6), 7225-7237.

[19] Salary, E., & Darvish Falehi, A. (2022). Innovative step-up direct current converter for fuel cell-based power source to decrease current ripple and increase voltage gain. ETRI Journal, 44(4), 695-707.

[20] Obe, D. O., Obe, C. T., Ugwuishiwu, C. H., Obe, P. I., Eneh, A. H., Odeh, C. I., & Obe, E. S. (2024). A single-phase, nine-level switched-capacitor-based inverter. Journal of Power Electronics, 1-12.

[21] Liang, G., Rodriguez, E., Farivar, G. G., Ceballos, S., Townsend, C. D., Gorla, N. B. Y., & Pou, J. (2022). A constrained inter submodule state-of-charge balancing method for battery energy storage systems based on the cascaded H-bridge converter. IEEE Transactions on Power Electronics, 37(10), 12669-12678.

[22] Rancilio, G., Dimovski, A., Bovera, F., Moncecchi, M., Falabretti, D., & Merlo, M. (2023). Service stacking on residential BESS: RES integration by flexibility provision on ancillary services markets. Sustainable Energy, Grids and Networks, 101097.

[23] Khalid, M., & Panigrahi, B. K. (2023). Decentralized Power Management in Multi BESS-PV Based Charging Infrastructure for EV With SoC Balancing. IEEE Transactions on Industry Applications.

[24] Saenko, I., & Kotenko, I.V. (2014). Design of Virtual Local Area Network Scheme Based on Genetic Optimization and Visual Analysis. Journal of Wireless Mobile Networks, Ubiquitous Computing, and Dependable Applications (JoWUA), 5(4), 86-102.

[25] Niazi, Y., Rajaei, A., Tehrani, V. M., Shasadeghi, M., Mobayen, S., & Skruch, P. (2023). A Switched-Capacitor Multi-Level Inverter With Variable Voltage Gain Based on Current-Fed Dickson Voltage Multiplier. IEEE Access, 11, 119352-119361.

[26] Yang, C. T., Chen, S. T., Lien, W. H., & Verma, V. K. (2019). Implementation of a Software-Defined Storage Service with Heterogeneous Storage Technologies. J. Internet Serv. Inf. Secur., 9(3), 74-97.